Transportation Research Part C 24 (2012) 19–35

Contents lists available at SciVerse ScienceDirect

Transportation Research Part C

journal homepage: www.elsevier.com/locate/trc

Optimal design of a non-linear controller for anti-lock braking system

Mehdi Mirzaei *, Hossein Mirzaeinejad

Research Laboratory of Mechatronics and Vibrations, Faculty of Mechanical Engineering, Sahand University of Technology, Tabriz, Iran

ARTICLE INFO

Article history:
Received 15 December 2010
Received in revised form 18 January 2012
Accepted 20 January 2012

Keywords:
Anti-lock brake system
Non-linear control
Optimal design
Optimum wheel slip

ABSTRACT

The most effective chassis control system for improving vehicle safety during severe braking is anti-lock braking system (ABS). In this paper, a nonlinear optimal controller is analytically designed for ABS by the prediction of the wheel slip response from a continuous nonlinear vehicle dynamics model. A new reference model for the wheel slip, which considers the effects of variations of tire normal load and tire/road condition, is proposed to be tracked by the controller. The main properties of the designed controller are evaluated and discussed by considering the important practical aspects of the slip control problem. The performed analysis along with the simulation results indicate that the designed controller with different special cases can successfully cope with the strong nonlinearity and realistic uncertainties existing in vehicle dynamics model. Meanwhile, a compromise between tracking accuracy and control energy can be easily made by the regulation of the weighting ratio, as a free parameter in the optimal control law.

1. Introduction

Recently, the development of chassis control systems for improving vehicle active safety has generated considerable interest in research community and automotive industries. Among these systems, the anti-lock brake system (ABS) is used to directly control the longitudinal dynamics of vehicle during braking (Furukawa and Abe, 1997).

The basic function of an ABS is to prevent the wheel form locking, and to regulate the longitudinal slip of the wheel at its optimum value in order to generate the maximum braking force. This permits the vehicle to achieve the shortest stopping distance during braking and at the same time improves the vehicle directional control and stability indirectly. In another application, since the ABS can regulate the longitudinal force acting independently on each wheel, it is used in the lower layer of vehicle dynamic control (VDC) system. In this system, the vehicle braking force is transversely distributed between the left and right wheels in a way that the external yaw moment required for stabilizing vehicle lateral dynamics is generated (van Zanten et al., 1998; Mirzaei et al., 2008). This strategy known as differential braking can be provided by the main parts of common anti-lock braking system.

The hard nonlinearities and modeling uncertainties existing in vehicle dynamics are the two main difficulties arising in the design of ABS controller. The first one is as a result of tire force saturation and the next one is mainly due to variations of road condition and vehicle parameters such as mass, center of gravity of the vehicle. Also, the un-modeled dynamics neglected in the course of modeling together with other practical limitations are considered as the un-structured uncertainties. A suitable controller for the ABS should successfully handle the nonlinearities and uncertainties existing in the vehicle model. On the other hand, the control law of ABS should be found in a way that the calculated control input, i.e. braking pressure, could be regulated easily so that one can keep it to the lowest possible value.

* Corresponding author. Address: P.O. Box 51335-1996, Sahand New Town, Tabriz, Iran. Tel.: +98 412 3444310; fax: +98 412 3444309.
E-mail addresses: mirzaei@sut.ac.ir, mehdi-mirzaei@hotmail.com (M. Mirzaei).

0968-090X/$ - see front matter © 2012 Elsevier Ltd. All rights reserved.
doi:10.1016/j.trc.2012.01.008

It is concluded from the above discussion that a non-linear controller with suitable robustness should be designed in an optimal way for the ABS. Many researchers have frequently applied the sliding mode control methods to ABS because of their potential to cope with nonlinearities and intrinsic robustness (Lin and Hsu, 2003; Unsal and Kachroo, 1999; Drakunov et al., 1995; Lee and Zak, 2002; Kazemi et al., 2000; Harifi et al., 2008; Park et al., 2006; Zheng et al., 2006; Song et al., 2007; Buckholtz, 2002). In these methods, the optimization is not used as the main procedure in finding the control law. Also, the chattering phenomenon is the undesirable effect of the sliding control in practice. Different techniques are introduced to reduce the chattering (Unsal and Kachroo, 1999; Harifi et al., 2008; Slotine and Li, 1991). In these methods, the discontinuous control law is smoothed to achieve a trade-off between control bandwidth and tracking precision. Also, some approaches such as higher order sliding mode controls (HOSM) can reduce the chattering and provide the higher accuracy than the conventional sliding modes. But they require higher control efforts and also the derivative of the control input is appeared in the derived control law (Bartolini et al., 1998).

In the following, the most important control methods used for the anti-lock braking systems are reviewed. Unsal and Kachroo (1999) used the sliding mode control to regulate the wheel slip at its optimum value. In their study, a PI-like controller was used near the switching surface instead of sign function to reduce chattering. Harifi et al. (2008) designed a sliding mode controller for ABS and used the integrated switching surface instead of sign function to reduce chattering. In this work, they had to find the proper bound of parametric uncertainties used in the designed control law. In another work, a fuzzy controller combined with the sliding mode control was introduced to reduce the dependency of controller on vehicle model (Lin and Hsu, 2003). Lee and Zak (2002) proposed a genetic neural fuzzy ABS controller that consists of a non-derivative neural optimizer and fuzzy-logic components. The non-derivative optimizer finds the optimal longitudinal wheel slip and then the fuzzy components compute the brake torque to track the optimal longitudinal wheel slip.

There are fewer optimal control laws for the ABS in the literature. Petersen (2003) designed a controller using gain scheduled LQR design method. A predictive optimal wheel slip controller based on a linearized vehicle model which was discretized via a bilinear transformation has been presented by Anwar and Ashraf (2002). These methods apply the linearized vehicle models and use on-line numerical optimization in finding the control law, whereas the use of non-linear model can broaden the valid range of operations as well as improve the accuracy of the controller. Also, numerical computation methods need online dynamic optimization and are not easy to solve and implement.

Generally, application of classic optimal control theories to the non-linear system requires that the derived non-linear two-point boundary value (TPBV) problem or Hamilton–Jacobi–Bellman (HJB) partial differential equations are solved. It is very difficult or even impossible to find an analytical solution for these problems.

In this paper, an optimal predictive approach is applied to design a nonlinear model-based controller for braking pressure. The proposed optimal control method is based on the predictive concept introduced by Lu (1995) for continuous nonlinear systems. In this method, a pointwise minimization performance index that penalizes the tracking error at the next instant, yet is not excessive, is used to find the current control input. The method analytically leads to a closed-form control law which is suitable to implement and the online numerical computations in optimization are not required (Lu, 1995; Mirzaei et al., 2008; Eslamian et al., 2007). In the development of this approach for the ABS, authors have already designed a nonlinear controller with increased robustness to track a constant wheel slip during braking for all road conditions (Mirzaeinejad and Mirzaei, 2010). In this earlier work, the weighting term of the control input is not included in the performance index to be minimized. In this case, referred to the cheap control, no limitation on the control input is assumed and the control law is obtained by minimizing only the tracking errors.

But, in the present study, the expensive control approach is considered. In this case, to achieve a minimum control effort and to make a compromise between the tracking error and control input, a complete optimization problem is defined. In this way, a weighted combination of tracking error and control expenditure is considered to be penalized in the performance index. Therefore, the optimal control law can be adjusted to keep the tracking error within the admissible range through the minimum control effort. At the rest, the main properties of the derived control law are analyzed and its different special cases are discussed. Following the performed analysis, the robustness of the proposed controller with respect to the important realistic uncertainties existing in practice is investigated. In this way, the effects of un-modeled dynamics and uncertain control gain due to fading the actuator dynamics are considered.

In another contribution of this study, a new reference model compatible with braking conditions is proposed for the wheel slip to be tracked by the controller. In this reference model, the variations of tire normal load and tire/road condition, which affect on the peak value of braking force, are considered. Also, according to the practical considerations, the new reference model is presented in a way that the slip controller is only active at the physical limits in which the wheel slip is beyond a threshold. As long as the slip resulting from the braking action of the driver is below the threshold, there is no control action. Tracking this model can generate the maximum braking force during braking on different roads and reduce the vehicle stopping distance remarkably.

It should be noted that the actual wheel slip is difficult to determine accurately due to a lack of practical means for directly measuring the linear speed of the tire center. Therefore, in many cases, the tire wheel slip is calculated from the estimated linear speed of the tire center and the measured angular speed of the tire, using various estimation methods (Ray, 1997; Gustafsson, 1997; Unsal and Kachroo, 1999). The estimation of road friction coefficient is also required to use in ABS controllers. The error caused by the estimation leads to some uncertainties which will be considered in the performance evaluation of the designed control system.

At the end of this paper, the effectiveness of the proposed controller in tracking the variable reference model is compared with a sliding mode controller, reported in the literatures, through simulations of various maneuvers.

2. System modeling

2.1. Wheel dynamics and tire force model

Basically, vehicle wheel dynamics is described by a quarter vehicle model as shown in Fig. 1. This model has been frequently used to design the controller for ABS (Unsal and Kachroo, 1999; Anwar and Ashraf, 2002; Park et al., 2006; Anwar, 2006; Mirzaeinejad and Mirzaei, 2010). The longitudinal velocity of the vehicle and the rotational speed of the wheel constitute the degrees of freedom for this model.

The governing equations for the motions of the wheel model are as follows:

$$\dot{V} = \frac{-F_x}{m_t} \tag{1}$$

$$\dot{\omega} = \frac{1}{I_t}(RF_x - T_b) \tag{2}$$

where R is the wheel radius, I_t is the total moment of inertia of the wheel, V is the longitudinal velocity of the vehicle, ω is the angular velocity of the wheel, T_b is the braking torque and F_x is the longitudinal tire force. Finally, m_t is the total mass of the quarter vehicle given by

$$m_t = \frac{1}{4}m_{vs} + m_w \tag{3}$$

In the above equation, m_{vs} is the vehicle sprung mass and m_w is the wheel mass. The longitudinal force acting on the tire depends on its normal load which has two components: a static component owing to the distribution of the vehicle mass, and a dynamic component owing to the load transfer during braking. Therefore, the tire normal load in the quarter model is given as follows:

$$F_z = m_t g - \frac{m_{vs}h_{cg}}{2l}\ddot{x} = m_t g - F_L \tag{4}$$

where l is the wheelbase, h_{cg} is the height of the sprung mass c.g. and F_L is the dynamic load transfer. In practice, the tire normal load is calculated by measuring the longitudinal acceleration $\ddot{x}$. But, in simulation study, F_z is calculated by substituting (1) into (4) and solving a nonlinear algebraic equation numerically.

During the braking, $V > R\omega$ and the wheel longitudinal slip is calculated as

$$\lambda = \frac{V - R\omega}{V} \tag{5}$$

Differentiating Eq. (5) with respect to time gives the derivative form

$$\dot{\lambda} = \frac{\dot{V}(1-\lambda) - R\dot{\omega}}{V} \tag{6}$$

Substituting (1) and (2) into (6) yields

$$\dot{\lambda} = -\frac{1}{V}\left[\frac{F_x}{m_t}(1-\lambda) + \frac{R^2F_x}{I_t}\right] + \left(\frac{RK_b}{VI_t}\right)P_b \tag{7}$$

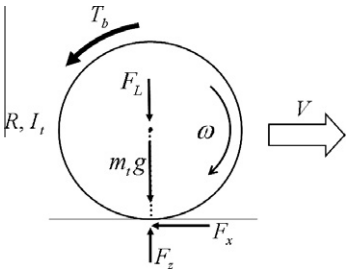

Fig. 1. Wheel free body diagram during braking.

In the above equation, the braking torque can be simply related to the pressure of the master cylinder with the formula $T_b = K_b P_b$ in which K_b is the braking system gain (Yi et al., 2000). This coefficient is uncertain due to fading effects of the actuator dynamics.

Eqs. (1) and (7) constitute the governing equations of motion in the state space form. The vehicle velocity V and the wheel longitudinal slip λ are the two state variables while P_b is the braking pressure which must be determined from the control law. In deriving the above equations, the effects of pitch and roll are neglected and straight-line braking with no steering is considered.

The longitudinal force F_x is described as a function of the longitudinal slip. If the longitudinal slip is small, the relationship between the longitudinal force and slip is linear, but with a further increase of the slip, the longitudinal force reaches a maximum at the certain value of the slip specified by tire-road adhesion and is saturated beyond that. In this case, the dynamic behavior of the vehicle will be non-linear. It is found that the saturation property of the tire force, as a basic cause of non-linear characteristics of vehicle motion, is the main reason of vehicle unsafe motions. The tire normal force as well as the road coefficient of friction strongly affect on the tire longitudinal force behavior.

In the present study, to account for the saturation property of the tire force, the non-linear Dugoff's tire model based on the friction ellipse idea has been used (Smith and Starkey, 1995). In this model, the relation for longitudinal force of tire is as follows

$$F_x = \frac{C_i \lambda}{1-\lambda} f(S) \tag{8}$$

where

$$f(S) = \begin{cases} S(2-S) & \text{if } S < 1 \\ 1 & \text{if } S > 1 \end{cases}$$

and

$$S = \frac{\mu F_z \left(1 - \varepsilon_r V \sqrt{\lambda^2 + \tan^2 \alpha}\right)(1-\lambda)}{2\sqrt{C_i^2 \lambda^2 + C_\alpha^2 \tan^2 \alpha}}$$

Here, C_i is the tire longitudinal stiffness, C_α is the cornering stiffness of the tire, μ is the road coefficient of friction, and ε_r is the road adhesion reduction factor. It should be noted that the straight-line braking with no steering is considered here and therefore a very small value for slip angle α will be assumed.

2.2. Reference model for wheel slip

The wheel slip reference model, which will be tracked by the ABS controller, should be selected in a way that the maximum braking force is achieved during hard braking on various roads. It is known that the longitudinal tire force is a non-linear function of the wheel slip. Meanwhile, the normal load of tire and the road coefficient of friction strongly affect on the behavior of tire force and its maximum value.

Fig. 2 shows the variations of the longitudinal tire force versus the wheel slip for different normal loads and surfaces. As seen in Fig. 2a, for a given surface, with increase in the value of normal load, the peak value of tire force increases and shifts to the right. The same results are found in Fig. 2b for different friction coefficients with a certain normal load. It is concluded that the location of optimum wheel slip depends on the braking conditions.

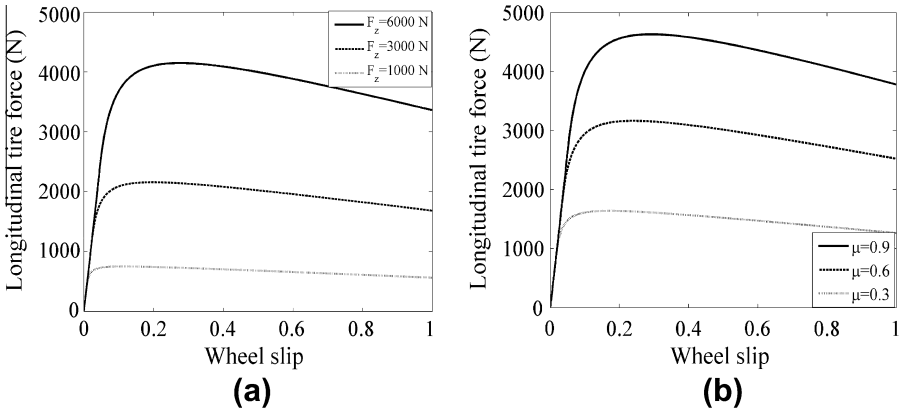

Fig. 2. Longitudinal tire force versus the wheel slip: (a) for different normal loads with $\mu = 0.8$ (b) for different surfaces with $F_z = 6000$ N.

During the braking, according to Eq. (4), the longitudinal acceleration causes normal load to shift from the rear to the front tires. Because of this dynamic load transfer, the normal load of the front tire, which is under study, increases and consequently affects on the optimum value of the wheel slip.

In many of the previous studies, the reference value of the wheel slip has been considered as a constant value between 0.1 and 0.2, typically 0.15 (Harifi et al., 2008; Anwar and Ashraf, 2002; Mirzaeinejad and Mirzaei, 2010). In the present study, in order to consider the effects of variations of normal load and friction coefficient, the optimum value of the wheel slip is calculated instantaneously by differentiating the longitudinal force described by the simplified Dugoff's tire model with respect to the wheel slip. In this way, the optimum wheel slip, λ_{opt}, can be found in terms of the tire normal load F_z and the road friction coefficient μ by online solving the following algebraic equation:

$$\left.\frac{\partial F_x}{\partial \lambda}\right|_{\lambda=\lambda_{opt}} = 0 \Rightarrow \quad (2-S)(1-\varepsilon_r U\lambda) - (2-2S)(1-\varepsilon_r U\lambda^2) = 0 \tag{9}$$

Note that in derivation of the above equation, the simplified Dugoff's tire model described by Eq. (8) with no slip angle is used. According to the Dugoff's model, $S < 1$ describes the nonlinear behavior of the tire force with respect to the wheel slip. The ABS controller will be active in this limit.

In the algebraic equation (9), the value of S is calculated in terms of the estimated values of μ and F_z. Therefore, in order to identify the optimal slip as a function of the friction coefficient, the road friction coefficient is first estimated from the measured vehicle data and then Eq. (9) is used. Because of the estimation error, the friction coefficient should be considered as an uncertain parameter. Note that different methods have been developed to estimate the friction coefficient (Ray, 1997; Gustafsson, 1997).

Fig. 3 illustrates the variation of optimum wheel slip, derived by the above equation, versus the normal load for two different surfaces.

In practice, the slip controllers are usually only active at the physical limits in which the wheel slip is beyond a threshold, typically $\lambda_{tr} = 0.1$. As long as the slip resulting from the braking action of the driver is below the threshold, there is no control action. In order to implement this feature and in order to include the transient response for the reference model of the wheel slip and to prevent a large tracking error at the beginning of the control action, the following first order system is considered as a desired model for the wheel slip

$$\lambda_d(t) = \lambda_{opt} + (\lambda_{tr} - \lambda_{opt})e^{-a(t-t_c)} \tag{10}$$

where λ_{opt} is the instantaneous optimum wheel slip, $a = 20$ is the time constant of the first order system (Harifi et al., 2008), λ_{tr} is the slip threshold and t_c is the time corresponding to λ_{tr}. During the braking, the designed controller will be active at time t_c when the wheel slip reaches λ_{tr}.

As a result, the desired braking system equipped to the controller will have the following response for the wheel slip during braking

$$\lambda_d(t) = \begin{cases} \lambda(t) & \text{when } \lambda < \lambda_{tr} \\ \lambda_{opt} + (\lambda_{tr} - \lambda_{opt})e^{-a(t-t_c)} & \text{when } \lambda \geqslant \lambda_{tr} \end{cases} \tag{11}$$

3. Control system design

3.1. Development of the control law

The nonlinear vehicle system dynamics described by Eqs. (1) and (7), can be written in the state space form by considering wheel slip as the output of the system

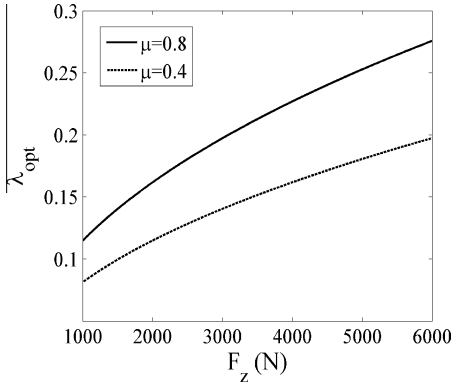

Fig. 3. Variation of optimum values of the wheel slip versus normal load for different surfaces.

$$\dot{x}_1 = f_1(\mathbf{x})) \tag{12}$$

$$\dot{x}_2 = f_2(\mathbf{x}) + \frac{RK_b}{I_t x_1} P_b \tag{13}$$

$$y = x_2 \tag{14}$$

where $\mathbf{x} = [V\lambda]^T$ is the state vector and y is the output. P_b representing the braking pressure is the control input. The nonlinear tire model given in Eq. (8), has been incorporated in f_1 and f_2.

The purpose of control system is to maintain the wheel slip, $x_2 = \lambda$, close to the desired response with the minimum braking pressure as the control energy. To achieve this aim, an optimal nonlinear control law should be developed for the design of wheel slip tracking controller. In this way, the nonlinear response of wheel slip for the next time interval, $\lambda(t+h)$, is first predicted by Taylor series expansion and then the current control $P_b(t)$ will be found based on continuous minimization of predicted tracking error. The predictive period h is a real positive number.

In order to find the current control, a pointwise minimization performance index that penalizes the tracking error at the next instant, yet is not excessive, and the current control expenditure is considered (Lu, 1995; Mirzaei et al., 2008)

$$J = \frac{1}{2} w_1 [\lambda(t+h) - \lambda_d(t+h)]^2 + \frac{1}{2} w_2 \left[P_b^2(t)\right] \tag{15}$$

where $w_1 > 0$ and $w_2 \geqslant 0$ are weighting factors indicating the relative importance of the corresponding terms.

First approximate $\lambda(t+h)$ by a kth-order Taylor series at t

$$\lambda(t+h) = \lambda(t) + h\dot{\lambda}(t) + \frac{h^2}{2!}\ddot{\lambda}(t) + \cdots + \frac{h^k}{k!}\lambda^{(k)}(t) \tag{16}$$

Now, the key issue is to choose the order k in a way that is suitable for the purpose of controller design on the basis of predictions. The expansion order, which specifies the highest order derivative of output used in the prediction, is determined by the control order plus the relative degree of the nonlinear system.

According to Eqs. (12)–(14), the system dynamics has the well-defined relative degree, $\rho = 1$, which is determined as the lowest order of the derivative of output λ in which the input P_b first appears explicitly (Slotine and Li, 1991).

On the other hand, to achieve a small control effort, the control order should be selected as low as possible. In this paper, the control order is limited to be zero so that the control effort will be a constant in the prediction interval

$$\frac{d}{d\tau} P_b(t+\tau) = 0 \quad \text{for } \tau \in [0, h] \tag{17}$$

This selection, i.e. zero control order, makes the derivatives of control input disappear in the prediction of the output and obtains relatively adequate performance for non-linear systems with lower relative degree (Lu, 1995; Chen et al., 2003). Generally, the control order is considered as a design parameter which makes a compromise between performance and input energy requirements.

Therefore, with the above reasoning, the first-order Taylor series is sufficient for the expansion

$$\lambda(t+h) = \lambda(t) + h\dot{\lambda}(t) \tag{18}$$

Substituting Eq. (13) into (18) yields

$$\lambda(t+h) = \lambda(t) + h\left(f_2 + \frac{RK_b}{VI_t} P_b\right) \tag{19}$$

Note that the arguments of function may be frequently dropped through the rest of paper for simplicity of notations.

The desired wheel slip can be expanded in the same manner as before

$$\lambda_d(t+h) = \lambda_d(t) + h\dot{\lambda}_d \tag{20}$$

Now, the expanded performance index can be obtained as a function of control input by substituting equations (19) and (20) into (15). The necessary condition for optimality is

$$\frac{\partial J}{\partial P_b} = 0 \tag{21}$$

which leads to

$$P_b(t) = -\frac{VI_t}{RK_b} \frac{\kappa}{h} [(\lambda - \lambda_d) + h(f_2 - \dot{\lambda}_d)] \tag{22}$$

where

$$\kappa = \frac{1}{1 + \beta\left(\frac{VI_t}{RhK_b}\right)^2} \tag{23}$$

and β is the weighting ratio

$$\beta = \frac{w_2}{w_1} \geqslant 0 \tag{24}$$

3.2. Evaluation of the optimal control law

In this section, the stability of the closed loop system is investigated along with the other properties of the designed controller. Meanwhile, the important roles of the free parameters, the predictive time h and the weighting ratio β, in the control law (22) are demonstrated. The dynamic performance of the controller is extremely sensitive to the value of these parameters.

From Eqs. (23) and (24), it is found that $0 \leqslant \kappa \leqslant 1$. This coefficient, referred to as reduction factor, provides the possibility of reducing the braking pressure by increasing the weighting ratio β. When $\beta = \infty$, then $\kappa = 0$ and $P_b = 0$. This case is considered as the expensive control and corresponds to the vehicle with no brakes. In contrast, the cheap control is related to the case of $\beta = 0$ in which $\kappa = 1$ and there is no reduction in control input.

In order to derive the closed loop system dynamics and analyze its stability in the presence of some modeling uncertainties, the control law (22), which is based on the nominal model, is applied to the actual model (13):

$$\dot{\lambda} = f_2 + g\left[\frac{-\kappa}{h\hat{g}}((\lambda - \lambda_d) + h(\hat{f}_2 - \dot{\lambda}_d))\right] \tag{25}$$

where

$$g = RK_b/VI_t \tag{26}$$

Note that the symbol "^" denotes the nominal model. Deviation of f_2 and g in the actual model from $\hat{f}_2$ and $\hat{g}$ in the nominal model can be a result of uncertainties in vehicle model and road condition.

Eq. (25) is rewritten as

$$(\dot{\lambda} - \dot{\lambda}_d) + \frac{g}{\hat{g}}\frac{\kappa}{h}(\lambda - \lambda_d) = (f_2 - \hat{f}_2) + \left(1 - \frac{g}{\hat{g}}\kappa\right)(\hat{f}_2 - \dot{\lambda}_d) \tag{27}$$

Hence, the tracking error dynamics of the wheel slip is obtained as follows

$$\dot{e} + \frac{g}{\hat{g}}\frac{\kappa}{h}e = (f_2 - \hat{f}_2) + \left(1 - \frac{g}{\hat{g}}\kappa\right)(\hat{f}_2 - \dot{\lambda}_d) \tag{28}$$

where e is the current tracking error of the wheel slip

$$e = \lambda - \lambda_d \tag{29}$$

The right hand side of Eq. (28) arises from both modeling uncertainty and reduction factor. These terms will always lead to some tracking errors. As a special case, when there is no reduction in control input nor modeling uncertainty, i.e. $\kappa = 1, f - \hat{f} = 0, g/\hat{g} = 1$, the tracking error dynamics of the wheel slip is obtained as follows

$$\dot{e} + \frac{1}{h}e = 0 \tag{30}$$

It is clear that the closed-loop system is linear and exponentially stable for any $h > 0$.

This version of the derived control law naturally leads to a special case of input/output linearization. According to error dynamics (30), as the initial wheel slip tracking error is zero, the perfect tracking of the wheel slip is maintained for all $t \in [0, t_f]$.

In studying the stability of the system in the presence of modeling uncertainties and reduction factor as the perturbed terms in Eq. (28), it is desirable to prove the boundedness of the error signal. In this way, since the unperturbed system described by Eq. (30) is linear and asymptotically stable, the system will be totally stable. The concept of total stability characterizes the ability of a system to withstand bounded persistent disturbances (Slotine and Li, 1991). It should be noted that the reduction factor κ, related to the free parameter β, is intentionally used to decrease the control input at the cost of some admissible tracking error. The value of this factor can be decreased to some extent, otherwise the perturbed term of Eq. (28) is more increased and therefore the wheel slip cannot follow the behavior of reference model adequately and the controller performance is lost.

Now, the upper and lower bounds of the error signal in the presence of the perturbed terms in Eq. (28) are found. According to Eqs. (7) and (13), the function f_2 which has the main role in the perturbed terms is expressed as

$$f_2(x) = -\frac{1}{V}\left[\frac{F_x}{m_t}(1-\lambda) + \frac{R^2 F_x}{I_t}\right] \tag{31}$$

As it is considered, f_2 is mainly affected by the tire force F_x which is defined as a saturated function. Deviation of f_2 from the nominal model $\hat{f}_2$ can be as a result of uncertainties in vehicle model and road condition. However, since the tire force F_x is played a major role in the dynamic behavior of the vehicle, the error in estimating f_2 is mainly influenced by the estimated friction force $\hat{F}_x$. If the estimation error on F_x is assumed to be bounded, the error of the function f_2 can be constrained (Zheng et al., 2006). It should be noted that the velocity V is decreased during braking and consequently the function f_2 is increased according to Eq. (31). As a result, when the vehicle speed approaches zero, f_2 tends to infinity. In order to prevent this problem and to limit the function f_2, the control action is usually conducted up to the point where the vehicle velocity is near to 5 m/s (Lin and Hsu, 2003). After that the ABS will be inactive and the ordinary braking system is performed to stop the vehicle.

From the discussion above, it is found that during the control action, there exist constant $F > 0$ and $\eta > 0$ such that

$$|f_2 - \hat{f}_2| \leqslant F, \quad |\hat{f}_2 - \dot{\lambda}_d| \leqslant \eta \tag{32}$$

Also, according to Eq. (26), the error of g is mainly due to the uncertainty in the actuator coefficient K_b. The uncertainty in the other parameters of g can deviate it from the nominal model. With definition of p as a percentage of the uncertainty of g

$$g = \hat{g} \pm p\hat{g} \Rightarrow \frac{g}{\hat{g}} = 1 \pm p \tag{33}$$

Applying (32) and (33) into the error dynamics (28) and solving the first-order differential equations with zero initial condition, similar to (Mirzaei et al., 2008), implies that the tracking error is bounded within

$$-e_m \leqslant e(t) \leqslant e_m \quad \text{for all } t \geqslant 0 \tag{34}$$

where

$$e_m = \frac{F}{\kappa(1 \pm p)}h + \left(\frac{1}{\kappa(1 \pm p)} - 1\right)h\eta \tag{35}$$

According to the above equation, the tracking error for the negative sign of p will be greater than that for the positive p. This means that when the actual g is less than the nominal $\hat{g}$, the tracking error increases.

By using (23), the bound of tracking error (35) can be stated in terms of the weighting ratio β

$$e_m = \frac{1}{1-p}\left[\left(\frac{\beta}{h}\right)\left(\frac{VI_t}{R}\right)^2(F+\eta) + h(F+\eta p)\right] \tag{36}$$

Eq. (36) shows that a combination of h and β/h affects on the wheel slip tracking error. In fact, the tracking error can be controlled by regulation of the free parameters h and β. Another combination of h and β/h is found in the time constant of the closed-loop system. According to the error dynamics (28), the term of time constant includes the following term

$$\frac{h}{\kappa} = h + \frac{\beta}{h}\left(\frac{VI_t}{RK_b}\right)^2 \tag{37}$$

The inverse of the above term, i.e. κ/h, is also seen as the controller gain in Eq. (22). Therefore, it is concluded that the dynamic performance of the controller including tracking accuracy, tracking rate (or time constant) and control energy strongly depends on both h and the ratio of β/h. It should be noted that the controller performance is more sensitive to β/h than h in the beginning of braking because of the large value of $(VI_t/R)^2$. During braking, while the velocity V approaches zero, the value of $(VI_t/R)^2$ is gradually reduced and consequently the effect of β/h on the tracking error will be decreased based on Eq. (36). This subject will be further investigated in simulation studies.

Now, the effects of model uncertainties and weighting ratio on the wheel slip tracking error are discussed separately. First, suppose $F \neq 0$, $p \neq 0$ and $\beta = 0$. In this case, the bound of tracking error owing to modeling uncertainties is

$$e_m = \frac{h}{1-p}(F + \eta p) \tag{38}$$

It is found that the error can be controlled by regulation of the free parameter h. A high degree of robustness in the presence of some modeling uncertainties is achievable through small value of h. Therefore, in order to decrease the tracking error in the absence of the weighting ratio β, the value of h should be decreased.

In another case, suppose $\beta \neq 0$ and $F = 0$, $p = 0$.

In this case, the tracking error owing to reducing the control input via the weighting ratio α is as follows

$$e_m = \frac{\beta}{h}\left(\frac{VI_t}{R}\right)^2 \eta \tag{39}$$

It is seen that the tracking error depends on the ratio of β/h. Hence, the free parameters β and h must be regulated simultaneously.

4. Simulation results

Simulation studies are conducted to evaluate the performance of the proposed controller in tracking the new reference model. The parameters of the vehicle model employed for computer simulation are given in Table 1.

The vehicle is considered to move at a speed of 90 km/h along a straight path on a flat dry road ($\mu = 0.8$). Fig. 4 shows the vehicle responses with and without control during braking. It is supposed that there is no modeling uncertainty. Also, the slip threshold considered in Eq. (11) is equal to $\lambda_{tr} = 0.1$ and the controller is active only when the wheel slip reaches this value. As long as the slip resulting from the braking action of the driver is below the slip threshold, there is no control action.

The results of Fig. 4 indicate that when a hard braking is applied to the vehicle without ABS, the wheel becomes locked and its angular speed becomes zero within a short period of time (about 0.7 s), while the linear speed of the tire center V is not zero and is only reduced from 25 m/s to 20 m/s. Therefore, the vehicle begins to slide and consequently results an unsafe condition. In contrast, Fig. 4c illustrates that for the controlled vehicle when the slip reaches the threshold value ($\lambda_{tr} = 0.1$), the controller becomes active and the wheel slip follows the response of the proposed reference model perfectly. This allows the wheel angular speed to closely follow the vehicle speed without locking (Fig. 4b). Note that, no modeling uncertainty is assumed in this case and the weighting ratio is given zero. Therefore, since the initial wheel slip tracking error is zero, according to error dynamics (30), the obtained response coincides with the desired response so that the wheel slip tracking error is zero and the perfect tracking is achieved (Fig. 4d). Also, Fig. 4e compares the braking pressures for the controlled and un-controlled vehicle.

In order to illustrate the effectiveness of the new reference model, proposed for the wheel slip to be tracked by the controller, the results are compared with those obtained by the previous reference models in which the optimum value of the wheel slip is considered constant, typically $\lambda_{opt} = 0.15$ (Harifi et al., 2008; Mirzaeinejad and Mirzaei, 2010), irrespective of normal load variations during braking and road conditions. The designed controller in tracking both reference models is active at the physical limit (beyond $\lambda_{tr} = 0.1$). The simulation results on a dry road ($\mu = 0.8$) are compared in Fig. 5. As seen in Fig. 5a, the optimum value of the front wheel slip is increased during braking because of the normal load transfer. Therefore, by tracking the variable reference model, the maximum brake force is applied to the wheel at any time during braking. This fact is illustrated in Fig. 5b. As it is seen, the stopping time is considerably reduced and leads to a reduction of about 1.5 m for the stopping distance. Note that, in the absence of modeling uncertainty and weighting ratio, the designed controller follows both reference models perfectly without any tracking errors (Fig. 5c), but with different control inputs (Fig. 5d). The performance indexes of the controller including the integral values of squared tracking error and control energy for different reference models are represented in Table 2. Tire/road conditions will also affect on the optimum values of the wheel slip during braking. Therefore, selecting a constant value for optimum wheel slip for different roads will not lead to the maximum longitudinal force during braking at any time. In contrast, consideration of the proposed reference model compatible with the variation of tire normal loads and tire/road conditions improves the controller performance in generating the maximum forces during braking.

Now, the robustness of the designed controller in the presence of some modeling uncertainties is evaluated. In this respect, it is assumed that the uncertainties have risen out of 10% uncertainty in total mass of the vehicle and 10% uncertainty in the friction coefficient. Considering the previous maneuver, the effect of this structured uncertainty is seen in Fig. 6 for different values of the prediction time h. The result indicates that the wheel slip tracking error due to modeling uncertainty is reduced with the decrease of prediction time h as stated by Eq. (39). Also, Fig. 6b shows that the braking pressure is increased with the decrease of prediction time h. The performance indexes of the controller including the integral values of the squared tracking error and control energy for different values of h are represented in Table 3.

In another simulation study, the previous condition is repeated but on a slippery road ($\mu = 0.4$). The same results as before can be seen in Fig. 7. It is considered that the braking pressure for the slippery road is achieved much less than for the dry road. For this reason, the sensitivity of the control signal to the free parameter h in the slippery road is less than the dry road.

It should be noted that, in the presence of uncertainties, the transient error is gradually increased because of the increasing behavior of the uncertainty term in Eq. (28). In order to limit the function f_2 and consequently the uncertainty term $(f_2 - \hat{f}_2)$ during braking, the control action is conducted up to the point where the vehicle velocity is near to 5 m/s.

Table 1
Parameters of the quarter vehicle model and the Dugoff tire model.

Wheel radius, R	0.326 m
Wheel base, l	2.5 m
Center of gravity height, h_{cg}	0.5 m
Wheel mass, m_w	40 kg
$\frac{1}{4}$ of vehicle sprung mass, $\frac{1}{4}$ m_{vs}	415 kg
Total moment of inertia of wheel, I_t	1.7 kg m^2
Tire longitudinal stiffness, C_i	50,000 N/rad
Cornering stiffness of the tire, C_α	30,000 N/unit slip
Road adhesion reduction factor, ε_r	0.015
Slip angle, α	0

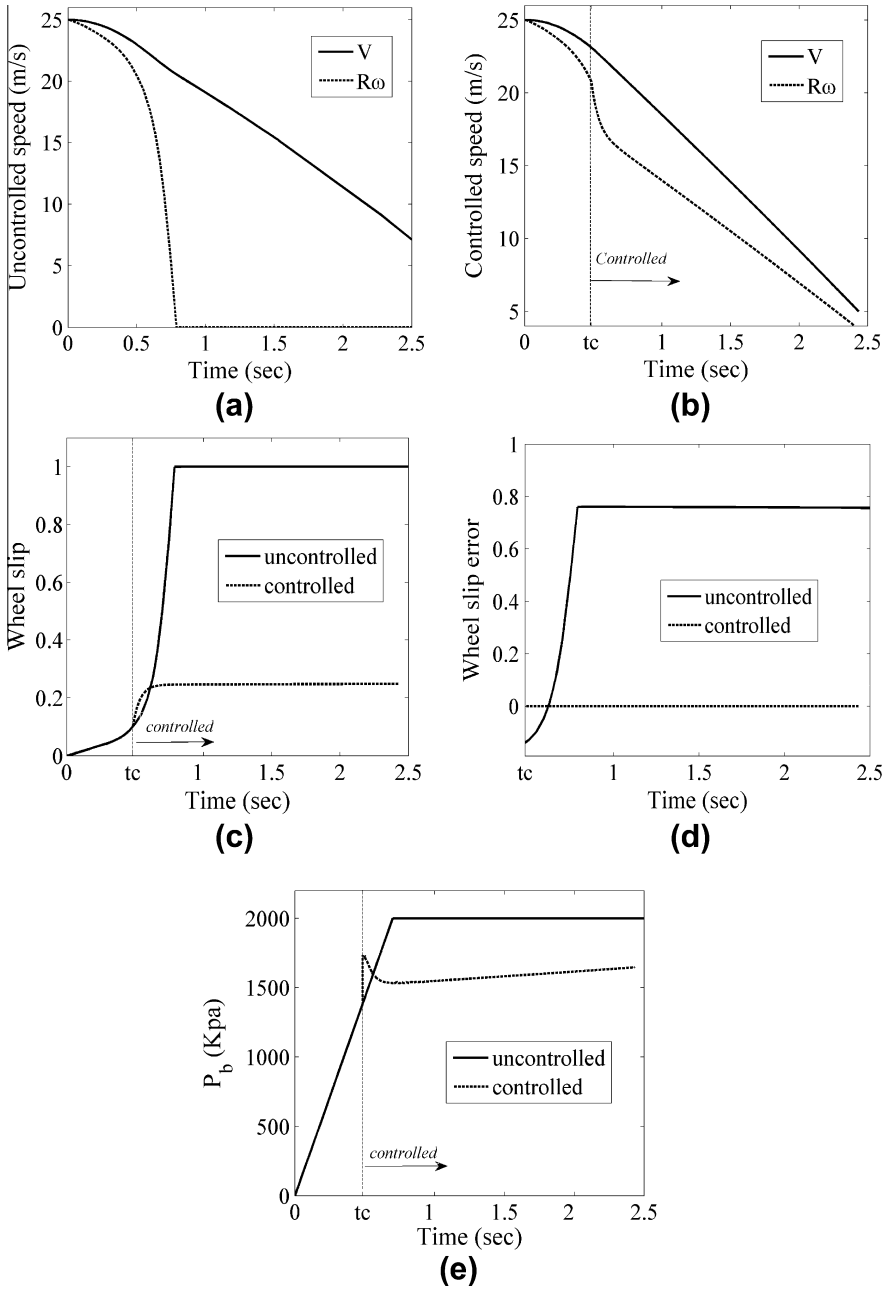

Fig. 4. Simulation results during braking with and without control: (a) wheel and vehicle speed (uncontrolled), (b) wheel and vehicle speed (controlled) (c) wheel slip (d) wheel slip tracking error (e) braking pressure.

In order to take into account the effect of the other practical uncertainties, 10% uncertainty in the wheel slip and 10% uncertainty in the actuator gain k_b are considered in addition to the previous parametric uncertainties. The first uncertainty is as a result of estimating error of the wheel slip and the second one is due to the fading effect of the actuator dynamics. The extra effect of these uncertainties in the tracking error and control energy on the dry road is evaluated in Fig. 8. As it is expected, the tracking error can be reduced with the decrease of prediction time h. The related results are represented in Table 4.

In the previous simulations, the weighting ratio β was taken to be zero and the special case of the controller (cheap control) was considered. To investigate the influence of the weighting ratio on the controller performance, Fig. 9 shows the wheel slip tracking errors and braking pressures for different values of β. Here, it is assumed that there is no modeling uncertainty, i.e. $F = 0$, $p = 0$.

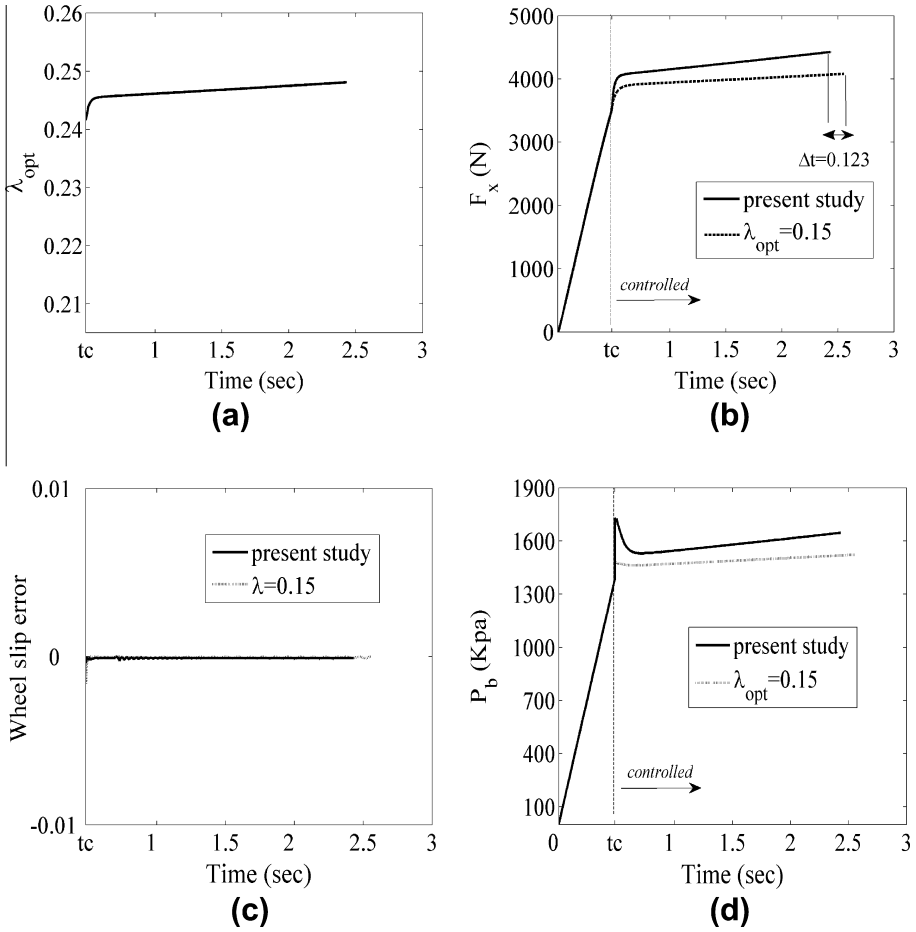

Fig. 5. Comparison of the controller performance in tracking the two different reference models on dry road: (a) variable optimum wheel slip (b) longitudinal tire force (c) wheel slip tracking error (d) braking pressure.

Table 2
Comparison of the controller performance with different reference models on dry road.

Optimum wheel slip	λ_{opt} = variable (Present study)	$\lambda_{opt} = 0.15$
$\int_0^{t_f} P_b^2 dt \times 10^{-6}$	4.231	3.971
$\int_0^{t_f} (\lambda - \lambda_d)^2 dt \times 10^{8}$	1.984	2.971
Stopping distance (m)	39.43	41.07

Fig. 9a illustrates that when $\beta = 0$, the wheel slip tracking error is zero and the perfect tracking is achieved according to Eq. (30). But, based on Eq. (39), with any increase in β, for a fixed h, the braking pressure decreases and the wheel slip tracking error increases. The performance indexes of the controller for different values of β and a fixed h are compared in Table 5. On the other hand, Table 6 explains that with the increase in h, for a fixed β, the braking pressure increases and the wheel slip tracking error decreases. These results confirming Eq. (39) demonstrate that the dynamic performance of the controller strongly depends on the ratio of β/h. It is seen in Fig. 9, the influence of β/h is gradually decreased during braking because the velocity V is decreased and consequently the amount of $(VI_t/R)^2$, which is the coefficient of β/h in Eq. (39), is reduced. The same results can be seen on a slippery road ($\mu = 0.4$) in Fig. 10. It is considered that the sensitivity of the control signal to the weighing ratio β in the slippery road is much less than the dry road.

In continuation of simulation studies, the performance of the proposed controller in the presence of both modeling uncertainty and weighting ratio is investigated. Fig. 11 shows the simulation results achieved in the presence of uncertainty for different values of β. The performance indexes are represented in Table 7.

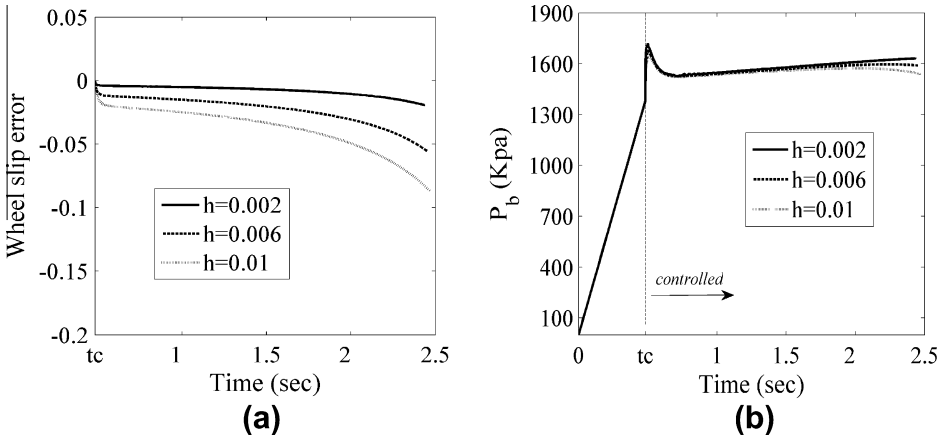

Fig. 6. Effect of prediction time h on the controller performance on dry road in the presence of uncertainties in the friction coefficient and vehicle mass: (a) wheel slip tracking error, (b) braking pressure.

Table 3
Controller performance for different values of h in the presence of uncertainties in vehicle mass and friction coefficient ($\beta = 0$).

h	0.002	0.006	0.01
$\int_0^{t_f} P_b^2 dt \times 10^{-6}$	4.22	4.17	4.14
$\int_0^{t_f} (\lambda - \lambda_d)^2 dt \times 10^4$	1.55	13	35
Stopping distance (m)	39.51	39.65	39.82

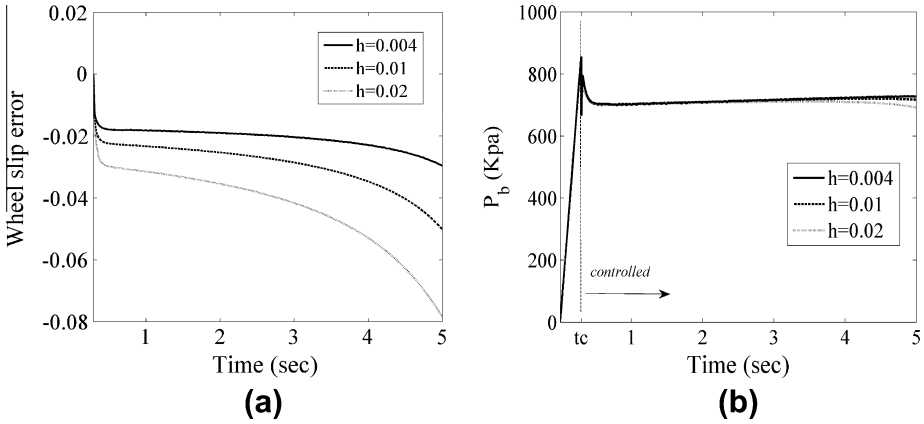

Fig. 7. Effect of prediction time h on the controller performance on slippery road in the presence of uncertainties in the friction coefficient and vehicle mass: (a) wheel slip tracking error, (b) braking pressure.

Generally, to adjust the controller, the prediction time h is firstly selected in a way that the best tracking with a smooth braking pressure is achieved for $\beta = 0$. Then, by increasing the weighting ratio β, the control input can be decreased at the cost of some tracking error. In this way, some control input limitations can be satisfied smoothly. It should be noted that in order to decrease the control input, the value of weighting ratio can be increased to some extent, otherwise the wheel slip cannot follow the behavior of reference model adequately and the controller performance is lost. It is found that when the input computed from the control law with a suitable value of weighting ratio exceeds the control bounds, the use of maximum control value can be the best choice which minimizes the performance index.

In order to complete the simulation studies, the dynamic performance of the proposed controller in this study, is compared with that of a sliding mode controller described in Appendix A. Because of the robust nonlinear characteristic of the sliding control, the special case of the proposed controller with $\beta = 0$ (cheap control) is adopted for the comparison. It should be noted that both controllers track the same reference models for the wheel slip.

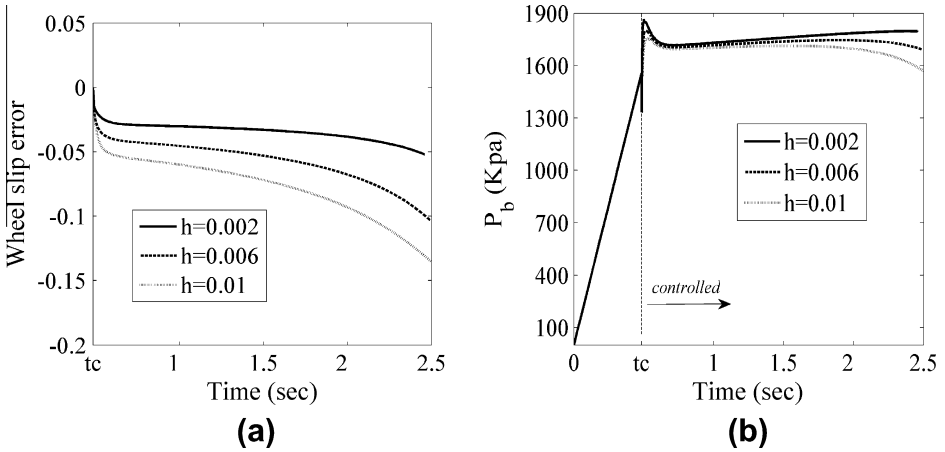

Fig. 8. Effect of prediction time h on the controller performance in the presence of uncertainties in the friction coefficient, vehicle mass, wheel slip and actuator gain: (a) wheel slip tracking error, (b) braking pressure.

Table 4
Controller performance for different values of h in the presence of uncertainties in vehicle mass, friction coefficient, wheel slip and actuator gain ($\beta = 0$).

h (s)	0.002	0.006	0.01
$\int_0^{t_f} P_b^2 dt \times 10^{-6}$	4.168	4.089	4.001
$\int_0^{t_f} (\lambda - \lambda_d)^2 dt \times 10^4$	24	72	140
Stopping distance (m)	39.77	40.12	40.57

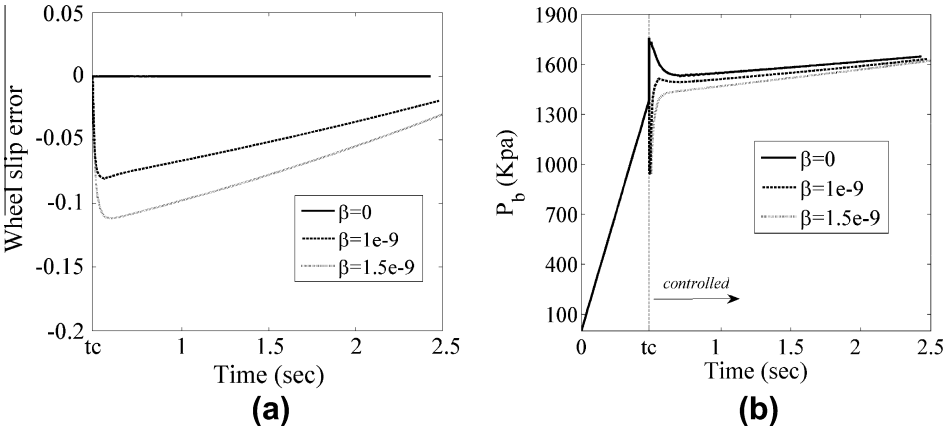

Fig. 9. Effect of weighting ratio β on the controller performance on dry road in the absence of modeling uncertainties: (a) wheel slip tracking error, (b) braking pressure.

Table 5
Controller performance for different values of β in the absence of uncertainty ($h = 0.002$ s).

β	0	1e−9	1.5e−9
$\int_0^{t_f} P_b^2 dt \times 10^{-6}$	4.230	4.121	4.042
$\int_0^{t_f} (\lambda - \lambda_d)^2 dt \times 10^4$	0.0002	58	126
Stopping distance (m)	39.45	40.26	41.05

Fig. 12 indicates a slightly larger tracking error for the sliding mode controller compared with the proposed controller during braking on a dry road. Note that, the design parameters of the sliding controller are regulated in a way that the lowest

Table 6
Controller performance for different values of h in the absence of uncertainty (β = 1.5e−9).

h	0.002	0.006	0.01
$\int_0^{t_f} P_b^2 dt \times 10^{-6}$	4.042	4.177	4.193
$\int_0^{t_f} (\lambda - \lambda_d)^2 dt \times 10^4$	126	15	5.44
Stopping distance (m)	41.05	39.75	36.61

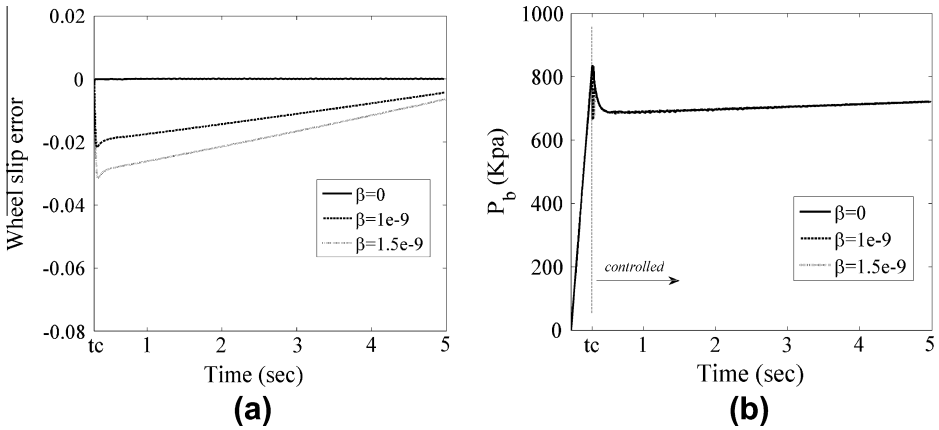

Fig. 10. Effect of weighting ratio β on the controller performance on slippery road in the absence of modeling uncertainties: (a) wheel slip tracking error, (b) braking pressure.

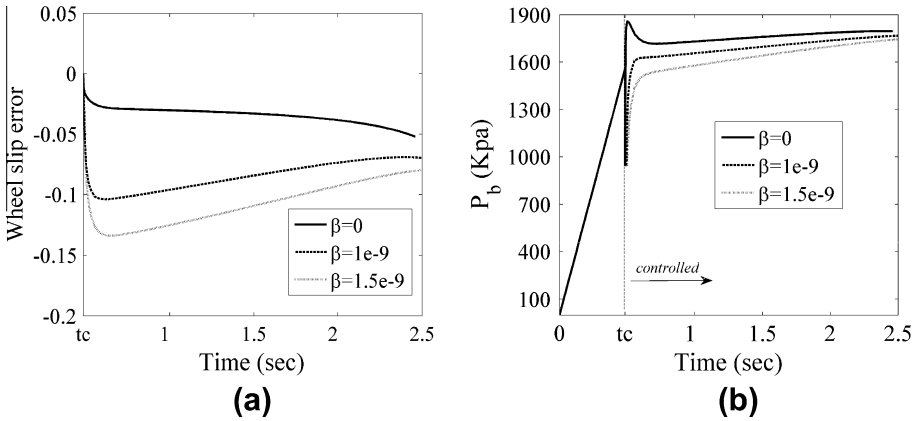

Fig. 11. Effect of weighting ratio β on the controller performance on dry road in the presence of modeling uncertainties: (a) wheel slip tracking error, (b) braking pressure.

Table 7
Controller performance for different values of β in the presence of uncertainty.

β	0	1e−9	1.5e−9
$\int_0^{t_f} P_b^2 dt \times 10^{-6}$	4.168	4.009	3.887
$\int_0^{t_f} (\lambda - \lambda_d)^2 dt \times 10^4$	24	149	247
Stopping distance (m)	39.77	41.11	42.36

tracking error is achieved. With any suitable changes in the regulation parameters, the error for both controllers cannot be decreased anymore and the responses begin to become oscillatory. The performance indexes of two controllers are also compared in Table 8.

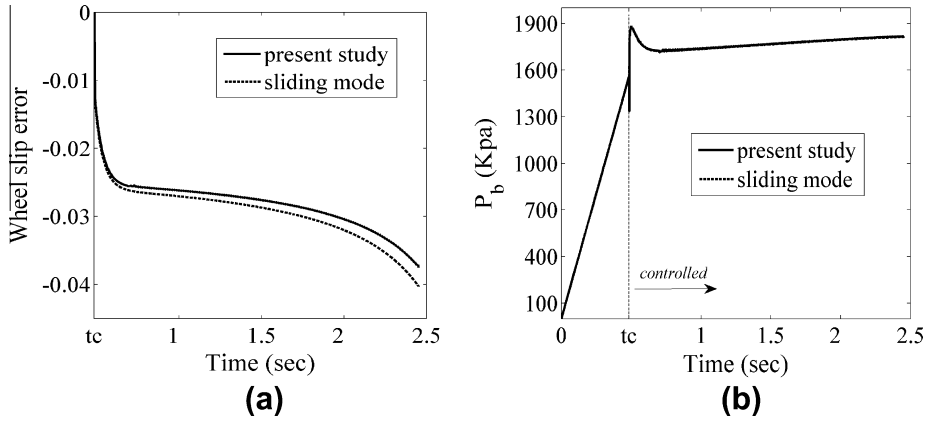

Fig. 12. Comparison of dynamic performances of the proposed controller and the sliding controller on dry road ($\mu = 0.8$): (a) wheel slip tracking error (b) braking pressure.

Table 8
Comparison of dynamic performances of two controllers on a dry road.

Method	Present study ($\beta = 0$)	Sliding mode
$\int_0^{t_f} P_b^2 dt \times 10^{-6}$	4.148	4.130
$\int_0^{t_f} (\lambda - \lambda_d)^2 dt \times 10^4$	16	17
Stopping distance (m)	39.70	39.72

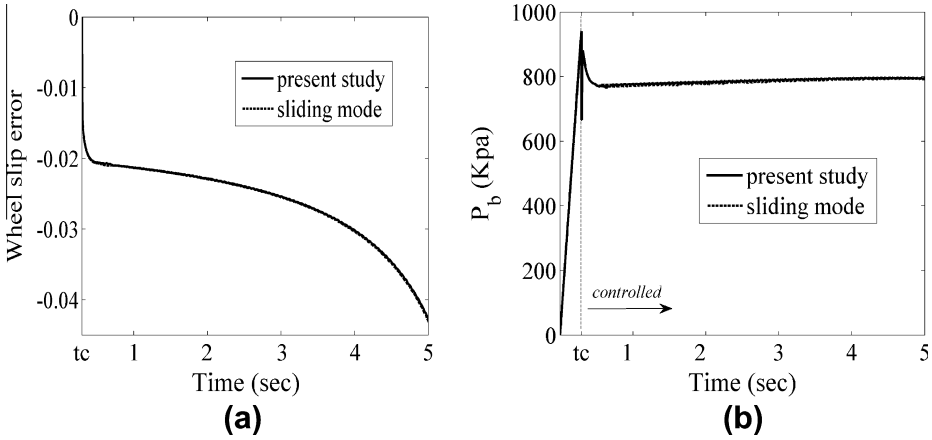

Fig. 13. Comparison of dynamic performances of the proposed controller and the sliding controller on slippery road ($\mu = 0.4$): (a) wheel slip tracking error (b) braking pressure.

Table 9
Comparison of dynamic performances of two controllers on a slippery road.

Method	Present study ($\beta = 0$)	Sliding mode
$\int_0^{t_f} T_b^2 dt \times 10^{-6}$	1.9274	1.9273
$\int_0^{t_f} (\lambda - \lambda_d)^2 dt \times 10^4$	34.1	34.5
Stopping distance (m)	76.73	76.74

Also, a comparison between the two controllers on a slippery road ($\mu = 0.4$) is presented in Fig. 13 and Table 9. The same results as dry road can be seen in this maneuver too.

5. Conclusions

An optimal nonlinear wheel slip tracking law is developed for ABS by the response prediction of a quarter vehicle model. To find the optimum wheel slip used in the reference model, the tire/road condition and tire normal load variations at any time during braking are considered. The proposed controller includes different features. It can handle the model nonlinearities and practical uncertainties successfully. The optimality of the control law provides the possibility of regulating the braking pressure easily. Also, the control law is developed in an analytical form which is easy to solve and implement. The method can be easily extended to the comprehensive vehicle models.

Appendix A

A1. Sliding mode control

A non linear braking pressure control law using sliding control theory was developed by researches as follows (Zheng et al., 2006; Buckholtz, 2002):

The sliding surface, S_s, is defined as

$$S_s = \lambda - \lambda_d \tag{40}$$

Taking time derivative of S_s and using Eq. (13) yields

$$\dot{S}_s = f_2 + \frac{RK_b}{I_t V} P_b - \dot{\lambda}_d \tag{41}$$

The best approximation $\hat{P}_b$ of a continuous control law that would achieve $\dot{S}_s = 0$ is thus

$$\hat{P}_b = -\frac{I_t V}{R\hat{K}_b}(\hat{f}_2 - \dot{\lambda}_d) \tag{42}$$

In order to satisfy sliding condition regardless of the uncertainty on the model f_2, a discontinuous term is added to $\hat{P}_b$:

$$P_b = \hat{P}_b - ksat\left(\frac{S_s}{\phi}\right) \tag{43}$$

k is selected as

$$k = \frac{I_t V}{R}(F + \eta), \tag{44}$$

where η is a strictly positive constant and ϕ is a design parameter denoting the boundary layer thickness. The saturation function can be defined as

$$sat\left(\frac{S_s}{\phi}\right) = \begin{cases} 1, & \frac{S_s}{\phi} > 1, \\ \frac{S_s}{\phi}, & -1 \leqslant \frac{S_s}{\phi} \leqslant 1, \\ -1, & \frac{S_s}{\phi} < -1. \end{cases} \tag{45}$$

References

Anwar, S., 2006. Anti-lock braking control of a hybrid brake-by-wire system. Proceedings of the Institution of Mechanical Engineers Part D – Journal of Automobile Engineering 220 (8), 1101–1117.

Anwar, S., Ashraf, B., 2002. A predictive control algorithm for anti-lock braking system. SAE paper 2002-01-0302.

Bartolini, G., Ferrara, A., Usai, E., 1998. Chattering avoidance by second-order sliding mode control. IEEE Transaction on Automatic Control 43 (2), 241–246.

Buckholtz, K.R., 2002. Reference input wheel slip tracking using sliding mode control. SAE Paper 2002-01-0301.

Chen, W.H., Balance, D.J., Gawthrop, P.J., 2003. Optimal control of nonlinear systems: a predictive control approach. Journal of Automatica 39 (4), 633–641.

Drakunov, S., Ozguner, U., Dix, P., Ashrafi, B., 1995. ABS control using optimum search via sliding modes. IEEE Transactions on Control System Technology 3 (1), 79–85.

Eslamian, M., Alizadeh, G., Mirzaei, M., 2007. Optimization-based non-linear yaw moment control law for stabilizing vehicle lateral dynamics. Proceedings of the Institution of Mechanical Engineers Part D – Journal of Automobile Engineering 221 (12), 1513–1523.

Furukawa, Y., Abe, M., 1997. Advanced chassis control systems for vehicle handling and active safety. Journal of Vehicle System Dynamics 28 (2), 59–86.

Gustafsson, F., 1997. Slip-based tire-road friction estimation. Journal of Automatica 6, 1087–1099.

Harifi, A., Aghagolzadeh, A., Alizadeh, G., Sadeghi, M., 2008. Designing a sliding mode controller for slip control of antilock brake systems. Journal of Transportation Research Part C 16 (6), 731–741.

Kazemi, R., Hamedi, B., Javadi, B., 2000. A new sliding mode controller for four-wheel anti-lock braking system (ABS). SAE Paper 2000-01-1639.

Lee, Y., Zak, S.H., 2002. Designing a genetic neural fuzzy antilock-brake-system controller. IEEE Transactions on Evolutionary Computation 6 (2), 198–211.

Lin, C.M., Hsu, C.F., 2003. Self-learning fuzzy sliding-mode control for antilock braking systems. IEEE Transactions on Control System Technology 11 (2), 273–278.

Lu, P., 1995. Optimal predictive Control of continuous nonlinear system. International Journal of Control 62 (3), 633–649.

Mirzaei, M., Alizadeh, G., Eslamian, M., Azadi, S., 2008. An optimal approach to non-linear control of vehicle yaw dynamics. Proceedings of the Institution of Mechanical Engineers Part I – Journal of Systems and Control Engineering 222 (4), 217–229.

Mirzaeinejad, H., Mirzaei, M., 2010. A novel method for non-linear control of wheel slip in anti-lock braking systems. Journal of Control Engineering Practice 18 (8), 918–926.
Park, E.J., Stoikov, D., Luz, L.F.D., Suleman, A., 2006. A performance evaluation of an automotive magnetorheological brake design with a sliding mode controller. Journal of Mechatronics 16, 405–416.
Petersen, I., 2003. Wheel slip control in ABS brakes using gain scheduled optimal control with constraints. Ph.D. thesis, Department of Engineering Cybernetics, Norwegian University of Science and Technology.
Ray, L.R., 1997. Nonlinear tire force estimation and road friction identification: simulation and experiments. Journal of Automatica 10, 1819–1833.
Slotine, J.J.E., Li, W., 1991. Applied Nonlinear Control. Prentice-Hall, Englewood Cliffs.
Smith, D.E., Starkey, J.M., 1995. Effect of model complexity on the performance of automated vehicle steering controllers: model development, validation and comparison. Journal of Vehicle System Dynamics 24 (2), 163–181.
Song, J., Kim, H., Boo, K., 2007. A study on an anti-lock braking system controller and rear-wheel controller to enhance vehicle lateral stability. Proceedings of the Institution of Mechanical Engineers Part D – Journal of Automobile Engineering 221, 777–787.
Unsal, C., Kachroo, P., 1999. Sliding mode measurement feedback control for antilock braking systems. IEEE Transactions on Control System Technology 7 (2), 271–281.
Van Zanten, A., Erhardt, R., Landesfeind, K., Pfaff, G., 1998. VDC system development and perspective. SAE Technical Paper, 980235.
Yi, J., Alvarez, L., Horowitz, R., Canudas de wit, C., 2000. Adaptive emergency barking control using a dynamic tire/road friction model. In: Proceeding of the 39th IEEE Conference on Decision and Control, Sydney.
Zheng, S., Tang, H., Han, Z., Zhang, Y., 2006. Controller design for vehicle stability enhancement. Journal of Control Engineering Practice 14 (12), 1413–1421.